

A Numerical Model for Muzzle Blast Flow Fields

T. D. TAYLOR and T. C. LIN
Vehicle Engineering Division
Engineering Group
The Aerospace Corporation
El Segundo, Calif. 90245

30 September 1980

Final Report

DISTRIBUTION STATEMENT A

Approved for public release;
Distribution Unlimited

DTIC QUALITY INSPECTED 3

APPROVED FOR PUBLIC RELEASE;
DISTRIBUTION UNLIMITED

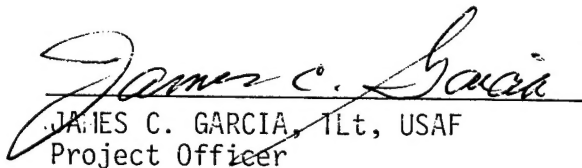
19970723 198

Prepared for
SPACE DIVISION
AIR FORCE SYSTEMS COMMAND
Los Angeles Air Force Station
P.O. Box 92960, Worldway Postal Center
Los Angeles, Calif. 90009

This final report was submitted by The Aerospace Corporation, El Segundo, CA 90245, under Contract F04701-79-C-0080 with the Space Division, Deputy for Technology, P.O. Box 92960, Worldway Postal Center, Los Angeles, CA 90009. It was reviewed and approved for The Aerospace Corporation by E.G. Hertler, Vehicle Engineering Division. The Air Force project officer was Lt. J.C. Garcia, SD/YLXT.

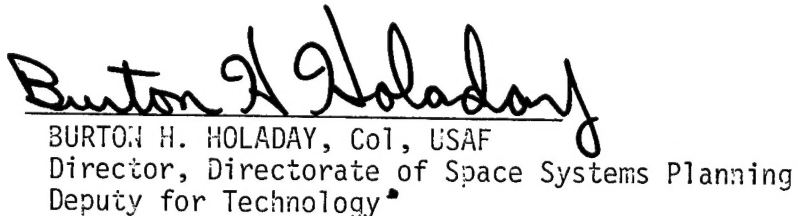
This report has been reviewed by the Public Affairs Office (PAS) and is releasable to the National Technical Information Service (NTIS). At NTIS, it will be available to the general public, including foreign nations.

This technical report has been reviewed and is approved for publication. Publication of this report does not constitute Air Force approval of the report's findings or conclusions. It is published only for the exchange and stimulation of ideas.


JAMES C. GARCIA, 1Lt, USAF
Project Officer


JOSEPH J. COX, JR., LtCol, USAF
Chief, Advanced Technology Division

FOR THE COMMANDER


BURTON H. HOLADAY, Col, USAF
Director, Directorate of Space Systems Planning
Deputy for Technology

UNCLASSIFIED

SECURITY CLASSIFICATION OF THIS PAGE (When Data Entered)

REPORT DOCUMENTATION PAGE		READ INSTRUCTIONS BEFORE COMPLETING FORM
1. REPORT NUMBER SD-TR-80-79	2. GOVT ACCESSION NO.	3. RECIPIENT'S CATALOG NUMBER
4. TITLE (and Subtitle) A NUMERICAL MODEL FOR MUZZLE BLAST FLOW FIELDS		5. TYPE OF REPORT & PERIOD COVERED Final August 1978-December 1978
		6. PERFORMING ORG. REPORT NUMBER TR-0080(9990)-3
7. AUTHOR(s) T. D. Taylor and T. C. Lin		8. CONTRACT OR GRANT NUMBER(s) F04701-79-C-0080
9. PERFORMING ORGANIZATION NAME AND ADDRESS The Aerospace Corporation El Segundo, Calif. 90245		10. PROGRAM ELEMENT, PROJECT, TASK AREA & WORK UNIT NUMBERS
11. CONTROLLING OFFICE NAME AND ADDRESS Space Division Air Force Systems Command Los Angeles, Calif. 90009		12. REPORT DATE 30 September 1980
		13. NUMBER OF PAGES 36
14. MONITORING AGENCY NAME & ADDRESS (if different from Controlling Office)		15. SECURITY CLASS. (of this report) Unclassified
		15a. DECLASSIFICATION/DOWNGRADING SCHEDULE
16. DISTRIBUTION STATEMENT (of this Report) Approved for public release; distribution unlimited.		
17. DISTRIBUTION STATEMENT (of the abstract entered in Block 20, if different from Report)		
18. SUPPLEMENTARY NOTES		
19. KEY WORDS (Continue on reverse side if necessary and identify by block number) Numerical Blast Wave Muzzle Blast Gas Flow		
20. ABSTRACT (Continue on reverse side if necessary and identify by block number) A numerical model is formulated to describe the details of the flow field produced by the firing of a gun or mortar. Godunov's scheme with an alternating direction implicit (ADI) procedure is employed to discretize and integrate the time-dependent Euler equations. Sample results are given for an M-16 rifle and a 4.2-in. mortar. Numerical results agree reasonably well with the existing experimental data.		

CONTENTS

1.	INTRODUCTION	5
2.	FORMULATION	9
3.	COMPUTATIONAL RESULTS	17
4.	SUMMARY	35

FIGURES

1.	Muzzle Flow Schematic	6
2.	Evaluation of Boundary State in Godunov Scheme	12
3.	Geometry for Muzzle Blast Calculation	13
4.	Propellant Gas Properties at Muzzle During Emptying	18
5.	Calculated Time History of Muzzle Blast and Mach Disc for M-16 Rifle	19
6.	Velocity Distribution Along the Centerline	20
7.	Pressure Distribution Along the Centerline	21
8.	Pressure Profile at $x/D = 5.2$	22
9.	Velocity Vector Projection	24
10a.	Constant Pressure and Density Profile for a 4.2-in. Mortar with Shell [Pressure (Muzzle Blast) $T = 0.999E-03$]	25
10b.	Constant Pressure and Density Profile for a 4.2-in. Mortar with Shell [Pressure (Muzzle Blast) $T = 0.203E-02$]	26
10c.	Constant Pressure and Density Profile for a 4.2-in. Mortar with Shell [$\rho \times 10^4$ (Muzzle Blast) $T = 0.203E-02$]	27
10d.	Constant Pressure and Density Profile for a 4.2-in. Mortar with Shell [Pressure (Muzzle Blast) $T = 0.364E-02$]	28
10e.	Constant Pressure and Density Profile for a 4.2-in. Mortar with Shell [$\rho \times 10^4$ (Muzzle Blast) $T = 0.364E-02$]	29
11a.	Constant Pressure and Density Profile for a 4.2-in. Mortar with No Shell [Pressure (Muzzle Blast) $T = 0.552E-03$]	30
11b.	Constant Pressure and Density Profile for a 4.2-in. Mortar with No Shell [Pressure (Muzzle Blast) $T = 0.191E-02$]	31

FIGURES (Continued)

11c. Constant Pressure and Density Profile for a 4.2-in. Mortar with No Shell [$\rho \times 10^4$ (Muzzle Blast) T = 0.191E-02]	32
11d. Constant Pressure and Density Profile for a 4.2-in. Mortar with No Shell [Pressure (Muzzle Blast) T = 0.323E-02]	33
11e. Constant Pressure and Density Profile for a 4.2-in. Mortar with No Shell [$\rho \times 10^4$ (Muzzle Blast) T = 0.323E-02]	34

1. INTRODUCTION

The gases discharged from a gun muzzle after firing determine the strength of the blast which affects firing crew safety and shell accuracy. In order to understand this phenomenon, a number of theoretical and experimental studies have been conducted. Extensive investigations of muzzle blast were carried out by Schmidt and his associates at BRL.^{1,2} A highly complex time-dependent flow field is noted in their flow visualizations results. For example, a schematic of the flow pattern is depicted in Fig. 1. It illustrates a large overexpansion jet, recompression shocks, contact surface, Mach disc, and free air blast. In early analytic work, Oswatitsch³ modeled the initial unsteady phase of this type of flow as a spherical blast. He applied the method of characteristics to calculate the blast field about the gun muzzle. Subsequently, he noted that in the region between the muzzle and the inward facing shock one can approximately model the flow by a steady jet theory. Erdos and Del Guidice⁴ have used this suggestion to evaluate the muzzle flow properties along the symmetry line.

¹Schmidt, E.M. and Shear, D.D., "The Flow Field About the Muzzle of an M-16 Rifle," BRL Report No. 1692, U.S. Army Ballistic Research Laboratory, Aberdeen Proving Ground, Md., Jan. 1974.

²Gion, E.J. and Schmidt, E.M., "Pressure Measurements on a Muzzle Brake Simulator," J. of Ballistics, Jan. 1978.

³Oswatitsch, K., "Flow Research to Improve the Efficiency of Muzzle Brakes, Part I through Part III," Muzzle Brakes, E.W. Hammer (ed.), Franklin Institute, 1949.

⁴Erdos, J. and Del Guidice, P., "Calculation of Muzzle Blast Flow-Fields," AIAA J., 13, 1975, p. 1048.

(This study was supported by the U.S. Army ARADCOM under Space Division, Air Force Systems Command Contract No. F04701-79-C-0080.)

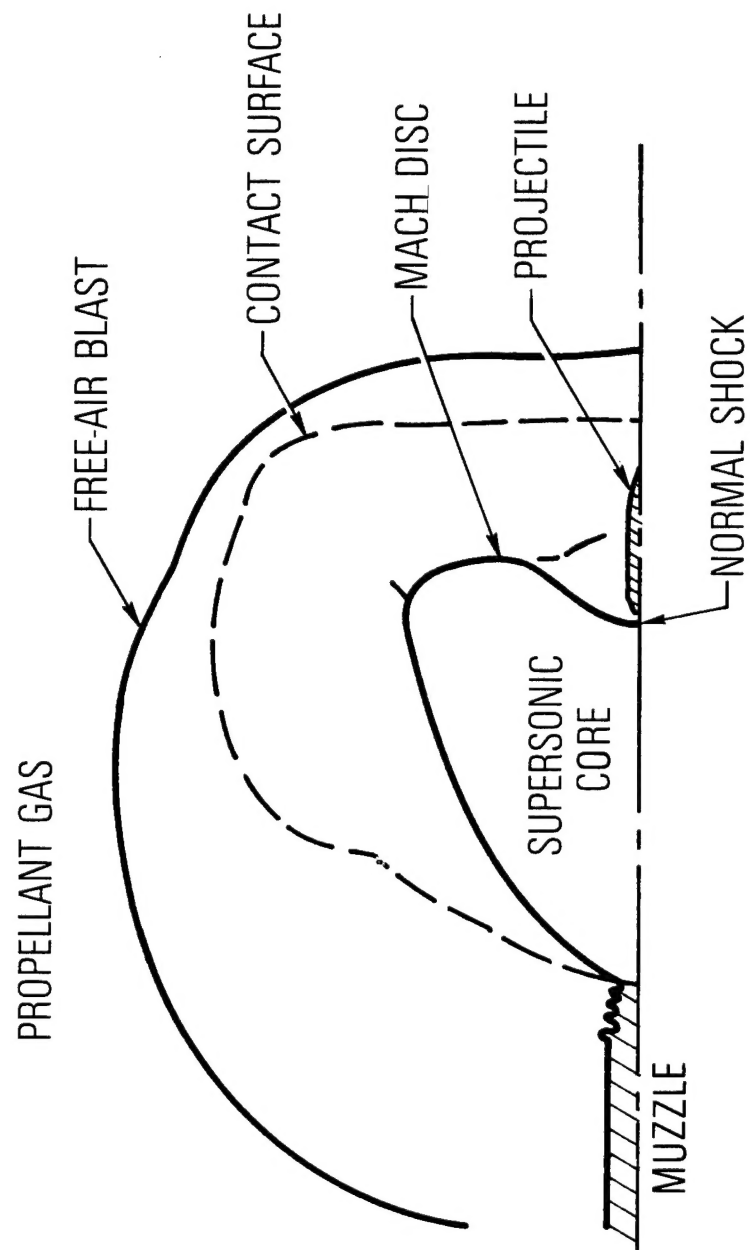


Fig. 1. Muzzle Flow Schematic

Recently, several attempts⁵⁻¹⁰ have been made to apply numerical methods to evaluate the fully two-dimensional or axisymmetric time-dependent muzzle flow field. Numerical calculations can predict the muzzle flow development in greater detail than in earlier analytic models. However, none of the calculations mentioned appear to have been compared to the existing experimental data in order to demonstrate their accuracy and validity.

As mentioned before, the muzzle blast flow field is complex and inherently unsteady. It provides a severe test of any numerical simulation technique due to the wide spectrum of flow conditions which exists as the transient flow field develops. However, the detailed simulation of the problem would considerably aid attempts to alleviate undesirable weapon characteristics such as recoil, noise, flash, and projectile dispersion. Until now, devices to suppress these undesirable characteristics are essentially designed by trial-and-error experimental programs.

⁵Taylor, T. D., "Calculation of Muzzle Blast Flow Fields," PA-R-4155, Picatinny Arsenal, Dover, N.J., Dec. 1970.

⁶Moore, G. R., "Finite Difference Calculations of the Free-Air Gun Blast About the Muzzle of a 5"/54 Naval Gun," Naval Weapons Laboratory, Report TR-2794, Sept. 1972.

⁷Ishiguru, T., "Finite Difference Calculations for Two-Dimensional Unsteady Expanding Flows," AIAA J., 10(2), Feb. 1972.

⁸Maille, F. H., "Finite Difference Calculations of the Free-Air Blast Field About the Muzzle and a Simple Muzzle Brake of a 105 mm Howitzer," Naval Weapons Laboratory, Report TR-2938, May 1973.

⁹Traci, R. M., Farr, J. L., and Liu, C. Y., "A Numerical Method for the Simulation of Muzzle Gas Flows with Fixed and Moving Boundaries," BRL-CR-161, U.S. Army Ballistic Research Laboratory, Aberdeen Proving Ground, Md., June 1974.

¹⁰Moretti, G., "Muzzle Blast Flow and Related Problems," AIAA paper 78-1190, Seattle, Wash., July 1978.

In this report, we investigate the phenomenon of muzzle blast by extending the numerical procedure used originally in Ref. 5. In this procedure we apply Godunov's method along alternating directions to solve the inviscid equations. The procedure works well except along the axis of symmetry where special precautions are necessary due to the extreme gradients in the flow. Details of the application and calculations results are presented in the following sections.

2. FORMULATION

In order to analyze the flow from the muzzle of a gun, we selected an inviscid flow model. Such a flow is described by the axisymmetric time-dependent Euler equations which can be written in the form

$$(\rho y)_t + (\rho v y)_y + (\rho u y)_x = 0$$

$$(\rho u y)_t + [y(p + \rho u^2)]_x + (\rho u v y)_y = 0$$

$$(\rho v y)_t + (\rho u v y)_x + [y(p + \rho v^2)]_y - p = 0$$

$$(\rho E y)_t + (\rho u H y)_x + (\rho v H y)_y = 0$$

where

$$E = e + 1/2 (u^2 + v^2)$$

e = specific energy of the fluid

$$H = E + P/\rho$$

t = time

x = direction along the axis of the gun

y = radial direction measured from the axis of symmetry

p = pressure

ρ = density

u = x velocity

v = y velocity

$$p = (\gamma - 1)\rho e$$

Godunov's scheme¹¹ was applied to discretize this governing system; however, we found that the nonlinear form of Godunov's method must be used, since the linear version of the scheme was discovered to be numerically unstable in regions of extreme gradients. Also, an ADI procedure was employed. The split equations took the following form:

Set I (for integration in the x direction)

$$\rho_{i,j}^{n+1/2} = \rho_{i,j}^n - \tau/h_x \left[RU_{i,j} - RU_{i-1,j} \right]$$

$$(\rho u)_{i,j}^{n+1/2} = (\rho u)_{i,j}^n - \tau/h_x \left[(P + RU^2)_{i,j} - (P + RU^2)_{i-1,j} \right]$$

$$(\rho v)_{i,j}^{n+1/2} = (\rho v)_{i,j}^n - \tau/h_x \left[RUV_{i,j} - RUV_{i-1,j} \right]$$

$$(\rho E)_{i,j}^{n+1/2} = (\rho E)_{i,j}^n - \tau/h_x \left[RUH_{i,j} - RUH_{i-1,j} \right]$$

Set II (for integration in the y direction)

$$\rho_{i,j}^{n+1} = \rho_{i,j}^{n+1/2} - \tau/h_y \left[RV_{i,j} - RV_{i,j-1} \right]$$

$$- \left[(RV_{i,j} + RV_{i,j-1}) / 2y_{i,j} \right] \tau$$

$$(\rho u)_{i,j}^{n+1} = (\rho u)_{i,j}^{n+1/2} - \tau/h_y \left[RUV_{i,j} - RUV_{i,j-1} \right]$$

$$- \left[(RUV_{i,j} + RUV_{i,j-1}) / 2y_{i,j} \right] \tau$$

¹¹ Godunov, S.K., "Finite Difference Method for Numerical Solutions of Equations of the Equations of Fluid Dynamics, " Mat. Sbornik, 47(89), No. 3, 1959.

$$\begin{aligned}
(\rho v)_{i,j}^{n+1} &= (\rho v)_{i,j}^{n+1/2} - \tau/h_y \left[(P + RV^2)_{i,j} \right] \\
&\quad - \left[(RV_{i,j}^2 + RV_{i,j-1}^2) / 2y_{i,j} \right] \tau \\
(\rho E)_{i,j}^{n+1} &= (\rho E)_{i,j}^{n+1/2} - \tau/h_y \left[(RVH)_{i,j} - (RVH)_{i,j-1} \right] \\
&\quad - \left[(RVH_{i,j} + RVH_{i,j-1}) / 2y_{i,j} \right] \tau
\end{aligned}$$

In these expressions each grid has an ordered pair of subscripts (i, j), with i denoting the x direction and j the y direction. The capital quantities (e.g., R, U, V, H, and P) refer to values of the flow variables on the cell edge which are computed by the nonlinear forms of Godunov's scheme (see Fig. 2).

Figure 3 illustrates the geometry and boundary conditions used in our formulation. In the present approach the shell is included in the analysis. Boundaries A, B, and C are solid boundaries with zero normal velocity, while boundary D is the shell base with a prescribed velocity u_g . Boundary E is an expanding grid line which moves outward just ahead of the muzzle blast. The grid is allowed to expand to a specified limit in x and y; then, "flow-through" boundary conditions are imposed along the line. This amounts to requiring each cell outside the boundary to have the same flow conditions in the outward normal direction as the cell inside the boundary.

Boundary F is the axisymmetric line across which there is no flow, and G is the muzzle exit condition. Initially, the conditions at G were specified as the muzzle launch conditions for all time. However, this was found to be incompatible with the real problem, since extreme pressures were generated in the muzzle blast which eventually caused the computations to become unstable. When the condition on G was relaxed and the actual flow

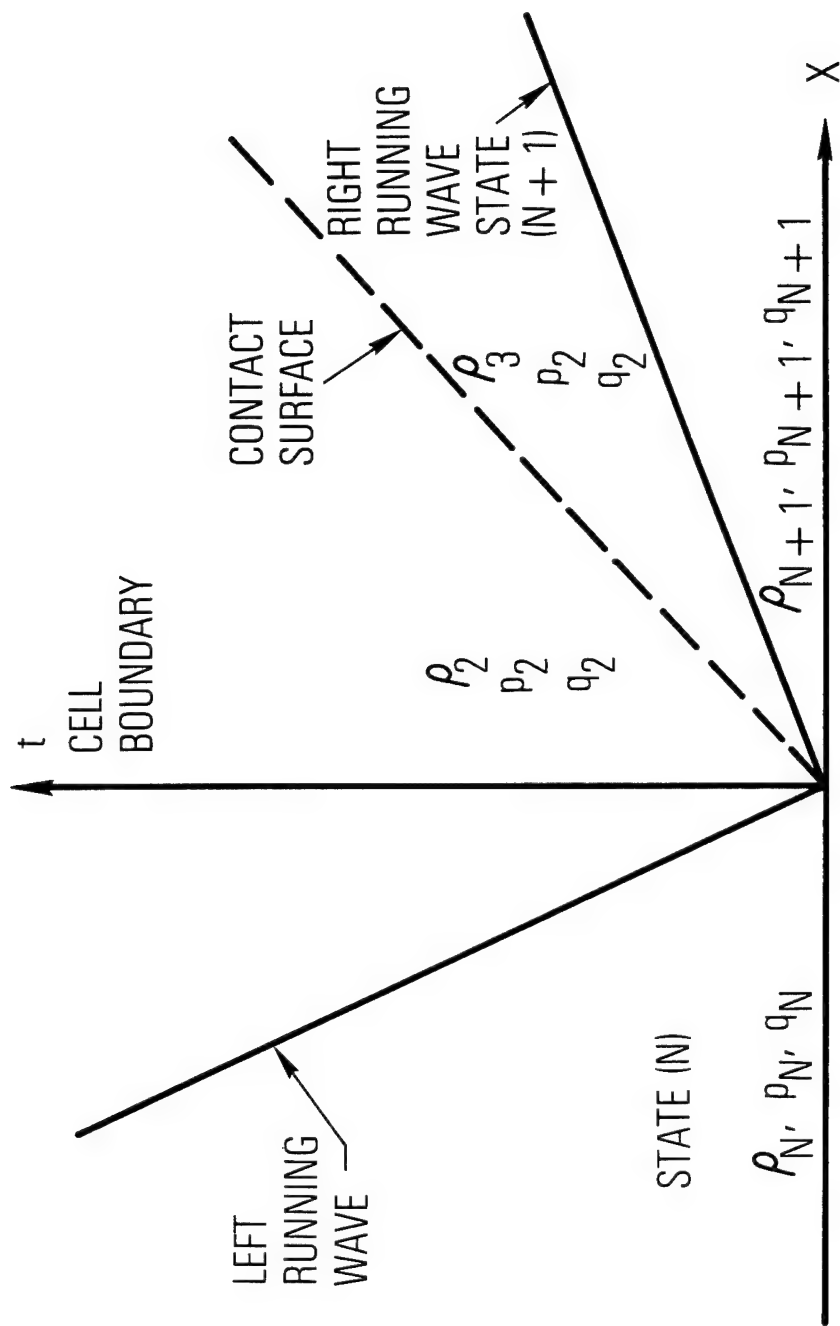


Fig. 2. Evaluation of Boundary State in Godunov Scheme

E= FREE STREAM UNDISTURBED PROPERTIES

C OR A= BOUNDARY CONDITIONS WITH $v = 0$

D= BOUNDARY CONDITION WITH u_s

F= SYMMETRY BOUNDARY CONDITION

B OR G= SPECIFIED BOUNDARY CONDITIONS AT MUZZLE EXIT

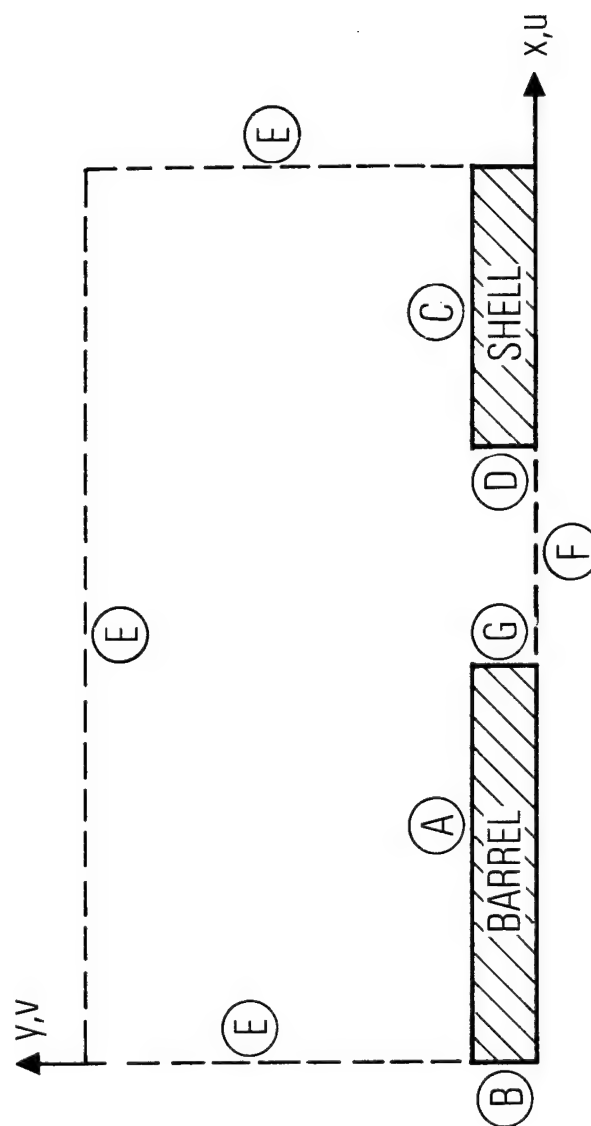


Fig. 3. Geometry for Muzzle Blast Calculation

within the gun was computed or specified in conjunction with the muzzle blast expansion, the results were very satisfactory. In the final configuration, the grid system considered flow both inside and outside the muzzle which is designated as boundary A.

The initial conditions for the problem consisted of ambient atmospheric conditions within the boundary AEC at launch. Within the gun ABFG, the conditions are prescribed as the launch conditions and must be provided by an independent interior ballistic calculation.

The velocity of the boundary D is prescribed as the shell launch velocity u_s . This boundary is advanced stepwise in time so that it is compatible with the step size Δx and the time Δt . Consequently, when $u \Delta t = \Delta x$, the projectile is advanced in the calculation one cell dimension. This was found to work satisfactorily and eliminated complicated program logic.

The calculation was started by integrating the split equations in the x direction for a half time step using the initial conditions and the boundary conditions. Results from these calculations were then used as initial conditions for the integration for a half time step in the y direction. The results are the full time step flow field. The cycle then is repeated to obtain the flow field at the next time step. The direction of integration for the first and second half time steps may be interchanged without altering the validity of the procedure.

Severe expansion gradients were encountered along the axis of symmetry and at the muzzle lip as the flow turned. In order to overcome these, we found it necessary not only to employ an implicit Godunov method, but also to modify the ADI method to compute the flow along the axis of symmetry. The problem along the axis occurred because the severe radial gradients of independent variables could not be accommodated adequately by the uncoupled x and y sweeps in ADI. As a result, we found it necessary to modify the x sweep of the radial velocity (v) equation so that the initial radial velocity in the cell next to the axis was a linear average across the cell rather than zero.

In order to simplify the study, we neglected the details of the flow about the projectile nose by assuming the projectile to be long and of uniform cross section. Also, the adiabatic gas constant was assumed to be constant at a value of $\gamma = 1.2$. These last two restrictions can be removed, but the character of the flow will not change.

As mentioned earlier, the flow field consists of an outer blast wave, a Mach disc, a contact surface, and jet shocks. It is difficult to treat these phenomena as distinct discontinuities, since the computer program logic can become tedious. Furthermore, the turbulent mixings will smear the inviscid flow discontinuities. As a result, the Godunov method is used to calculate these quantities without explicit fitting. Recently, Sod¹² and, previously, Taylor, et al.¹³ demonstrated that Godunov's scheme is particularly suitable for computing flows with embedded compression shocks and contact surfaces. In fact, the results of these two studies indicate that the Godunov scheme is preferable in most cases over higher order finite difference methods such as LAX-Wendroff and MacCormack. The reason for this may be explained by Moretti in his recent derivation of what he terms the "Lambda scheme."¹⁴ Moretti points out that methods which take into account the physics of the flow in their application tend to perform better than methods derived solely on the basis of a mathematical accuracy. As a result, he suggests that the Lambda scheme, which incidentally is very similar to the Godunov approach is superior to the classical finite difference methods.

¹²Sod, G.A., "A Survey of Several Finite Difference Methods for Systems of Nonlinear Hyperbolic Conservation Laws," J. Computational Physics, 27, 1978, pp. 1-31.

¹³Taylor, T.D., Masson, B.S., and Ndefo, E., "A Study of Numerical Methods for Solving Viscous and Inviscid Flow Problems," J. of Comp. Phys., 9(1), Feb. 1972.

¹⁴Moretti, G., "The λ -difference," J. Computers and Fluids, 7(3), Sept. 1979, pp. 191-206.

3. COMPUTATIONAL RESULTS

The mathematical model described above was incorporated into a computer program for the CDC 7600. Calculations were performed for the muzzle blast from an M-16 rifle for the purpose of comparison with the experimental results of Schmidt,¹ from whom the initial conditions in the gun were obtained. Figure 4 depicts Schmidt's data on muzzle pressure and flow exit velocity. For these data,¹ the muzzle diameter is $D = 5.56$ mm and the shell velocity is $U_s = 3100$ ft/sec. With these data used as input, the inviscid equations were numerically integrated to obtain the time history of the flow. The time histories of the Mach disc and blast wave equations are illustrated in Fig. 5. Also shown are the data of Schmidt.¹ The analytical results agree reasonably well with the experimental measurements. Note that the blast wave motion appears to follow a power law, i.e.

$$X_{\text{blast}}/D \sim (t U_s/D)^{0.605}$$

This seems to support the strong blast wave theory which predicts that the spherical blast obeys $X \sim t^{0.6}$. The centerline static pressure and velocity distribution at $t = 230$ μ sec are given in Figs. 6 and 7, respectively. Schmidt's experimental results also are shown. A tremendously large pressure decrease at the muzzle exit is discerned in Fig. 7. Any stable numerical scheme must properly take into account this significant pressure drop.

The pressure profile versus Y/D at $X/D = 5.2$ at various times is illustrated in Fig. 8. The position of the outer blast wave and inner jet shock can be identified in this figure. It should be pointed out that the lateral jet shock location at $t = 352$ μ sec and 233 μ sec is very close (i.e., $Y/D \sim 13$). Also, the numerical results (e.g., pressure) with a "shock-capturing" technique have little numerical oscillations or wiggles across the shock and contact surface discontinuities.

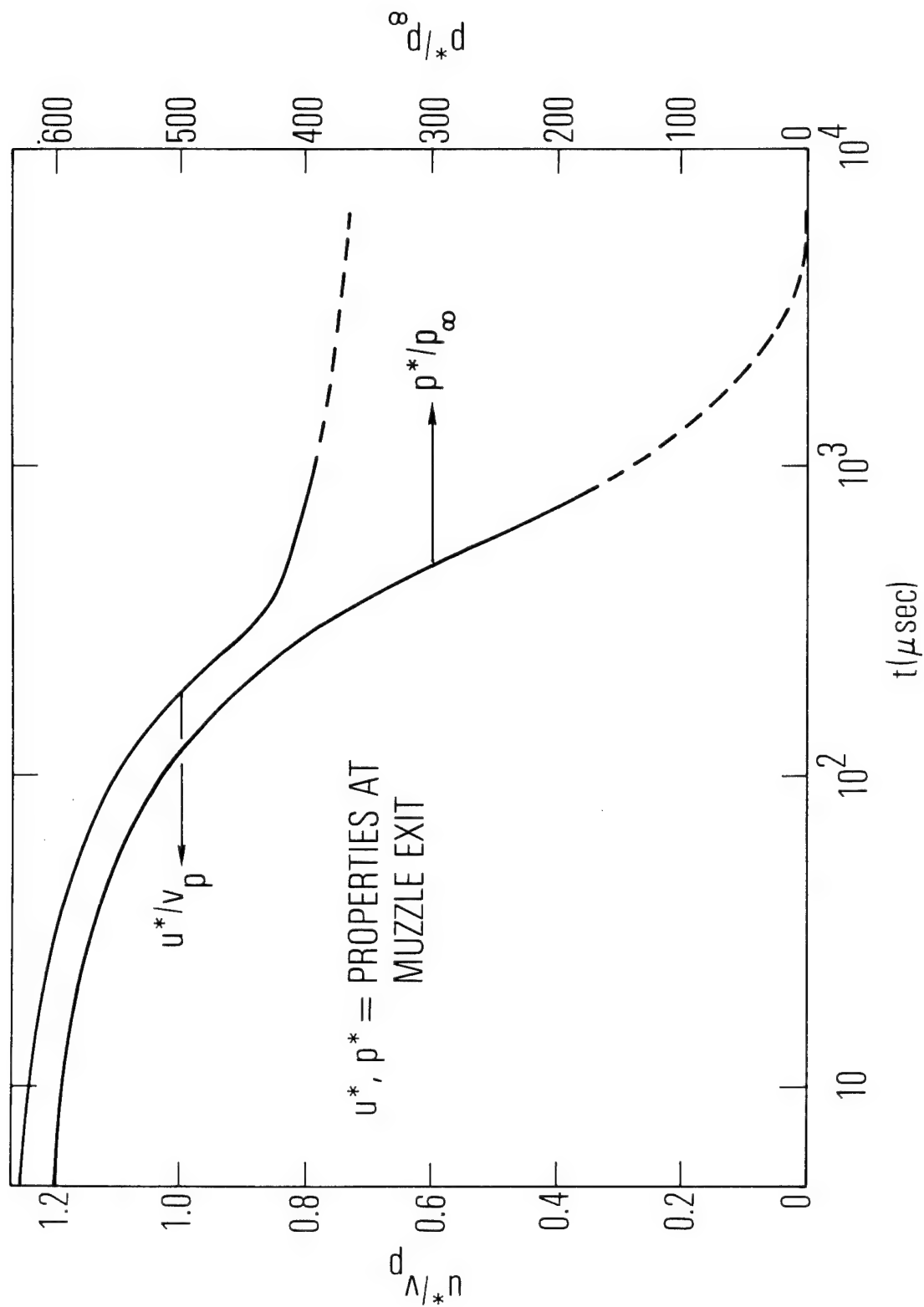


Fig. 4. Propellant Gas Properties at Muzzle During Emptying

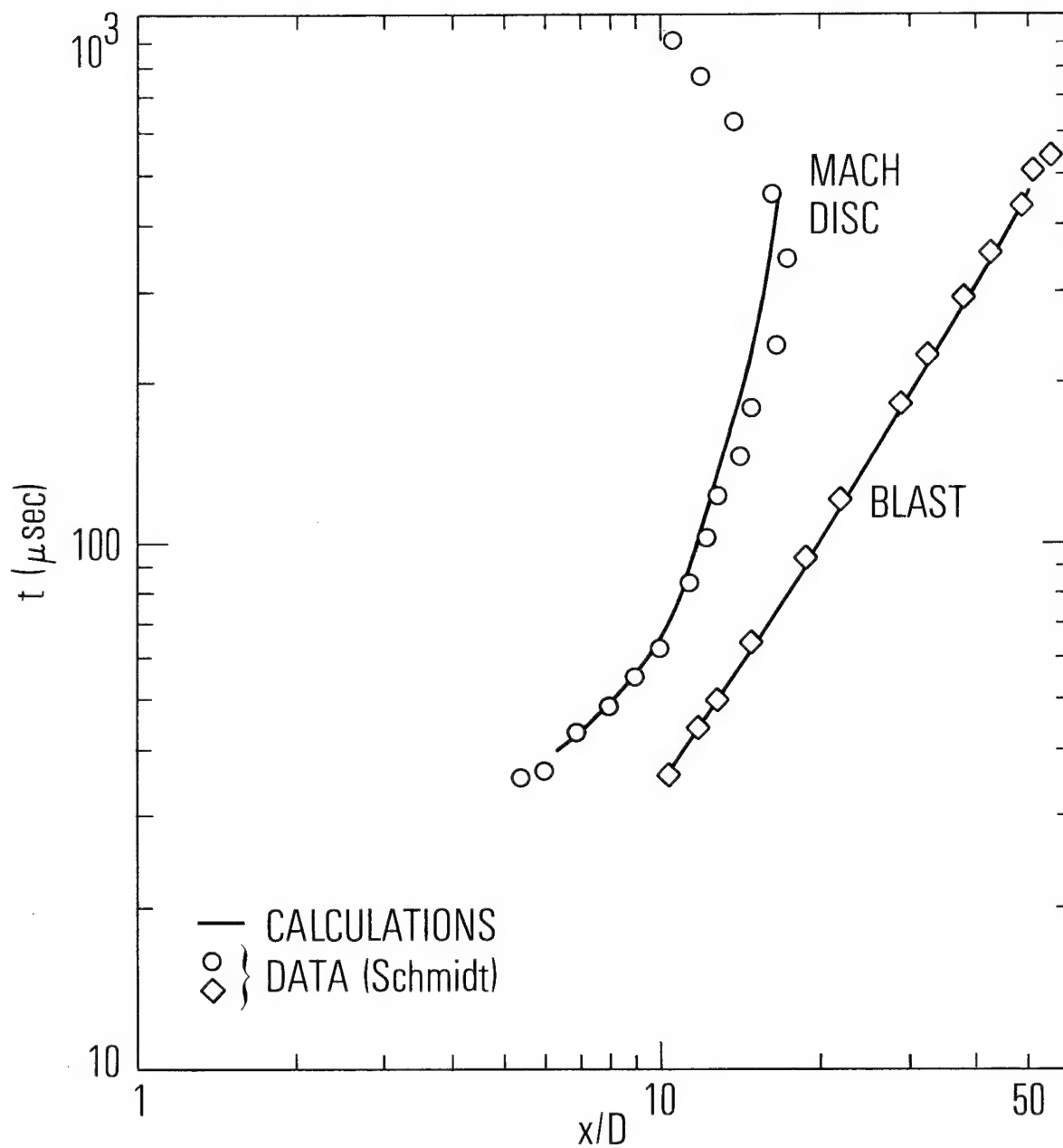


Fig. 5. Calculated Time History of Muzzle Blast and Mach Disc for M-16 Rifle

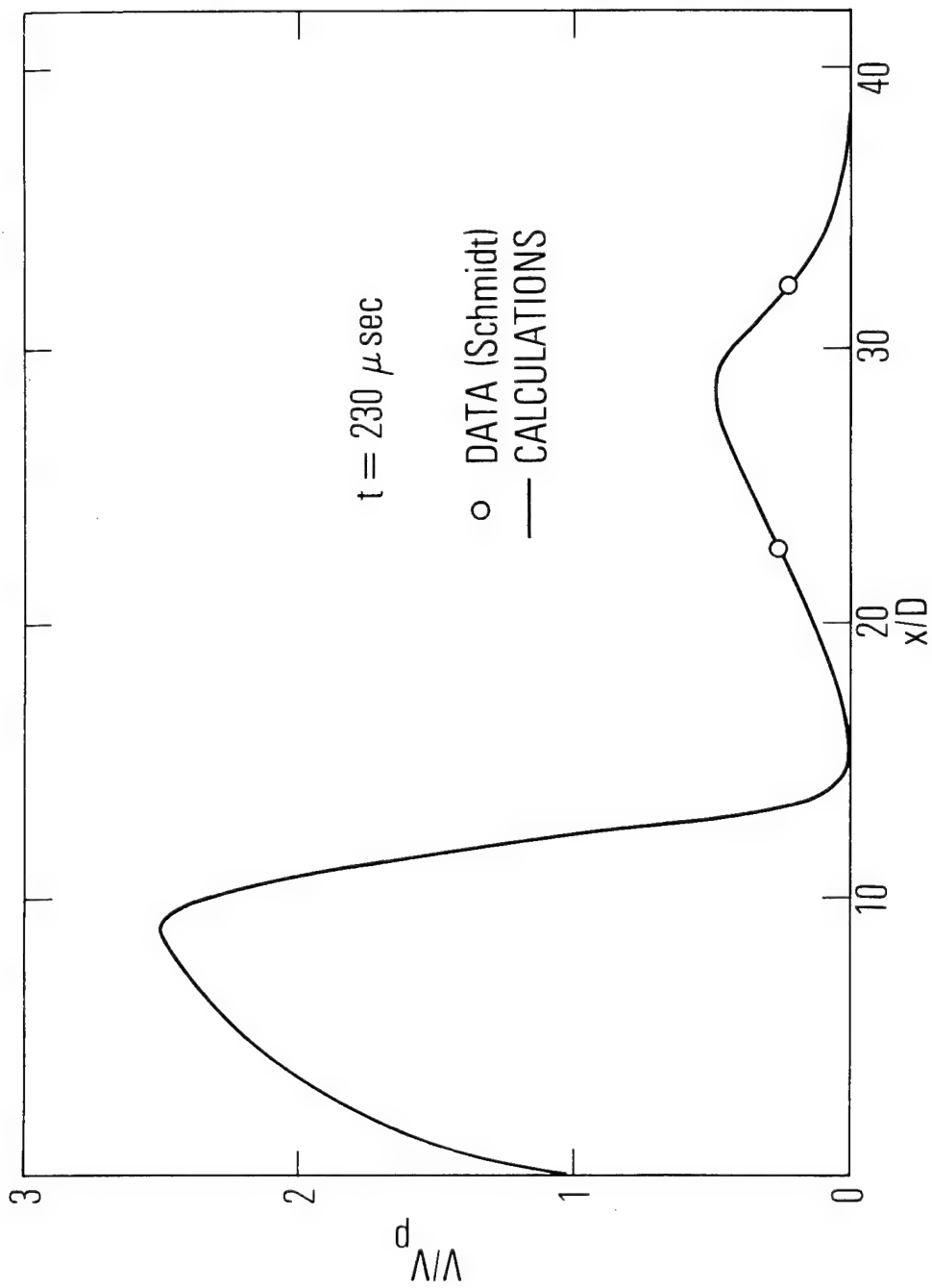


Fig. 6. Velocity Distribution Along the Centerline

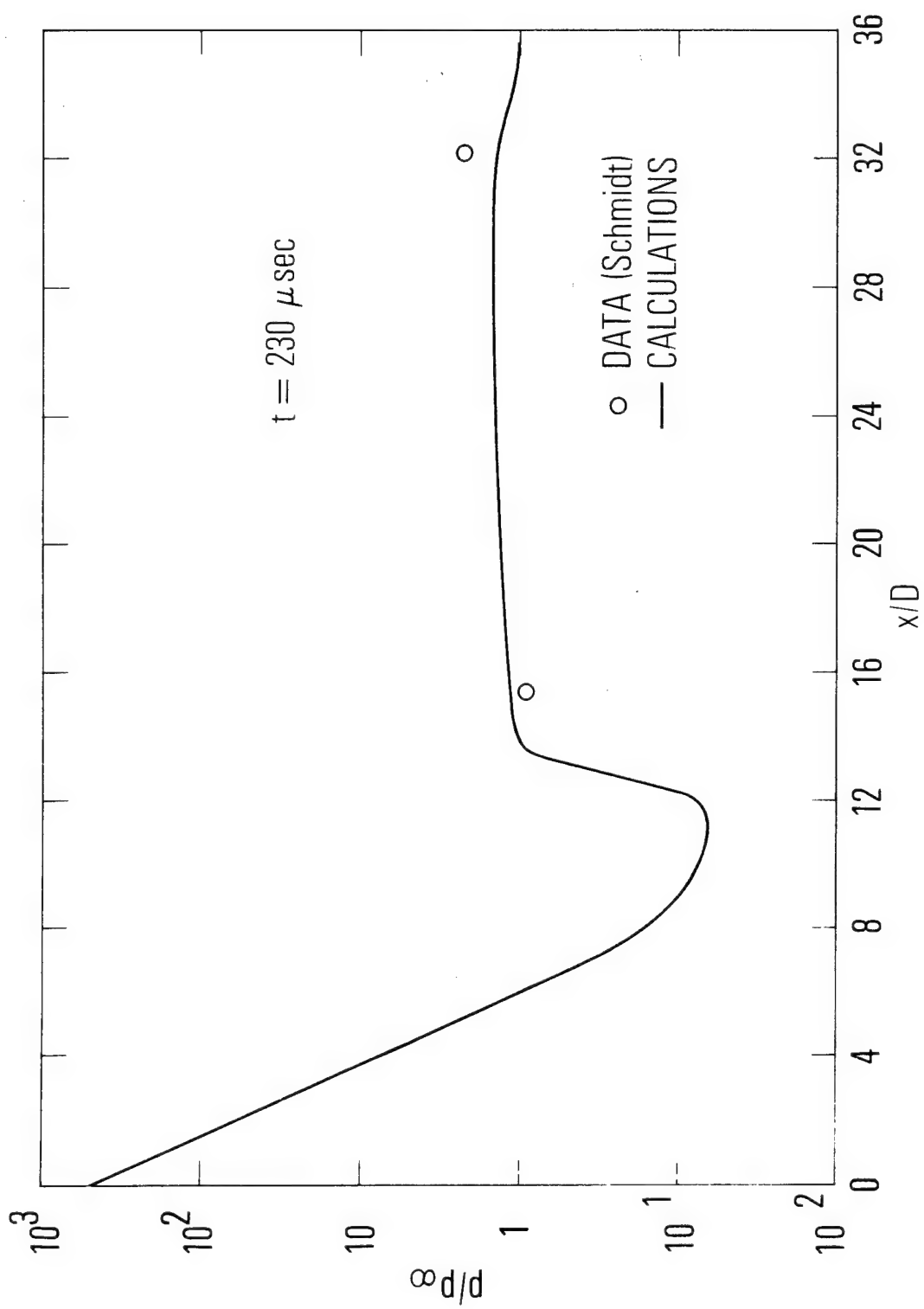


Fig. 7. Pressure Distribution Along the Centerline

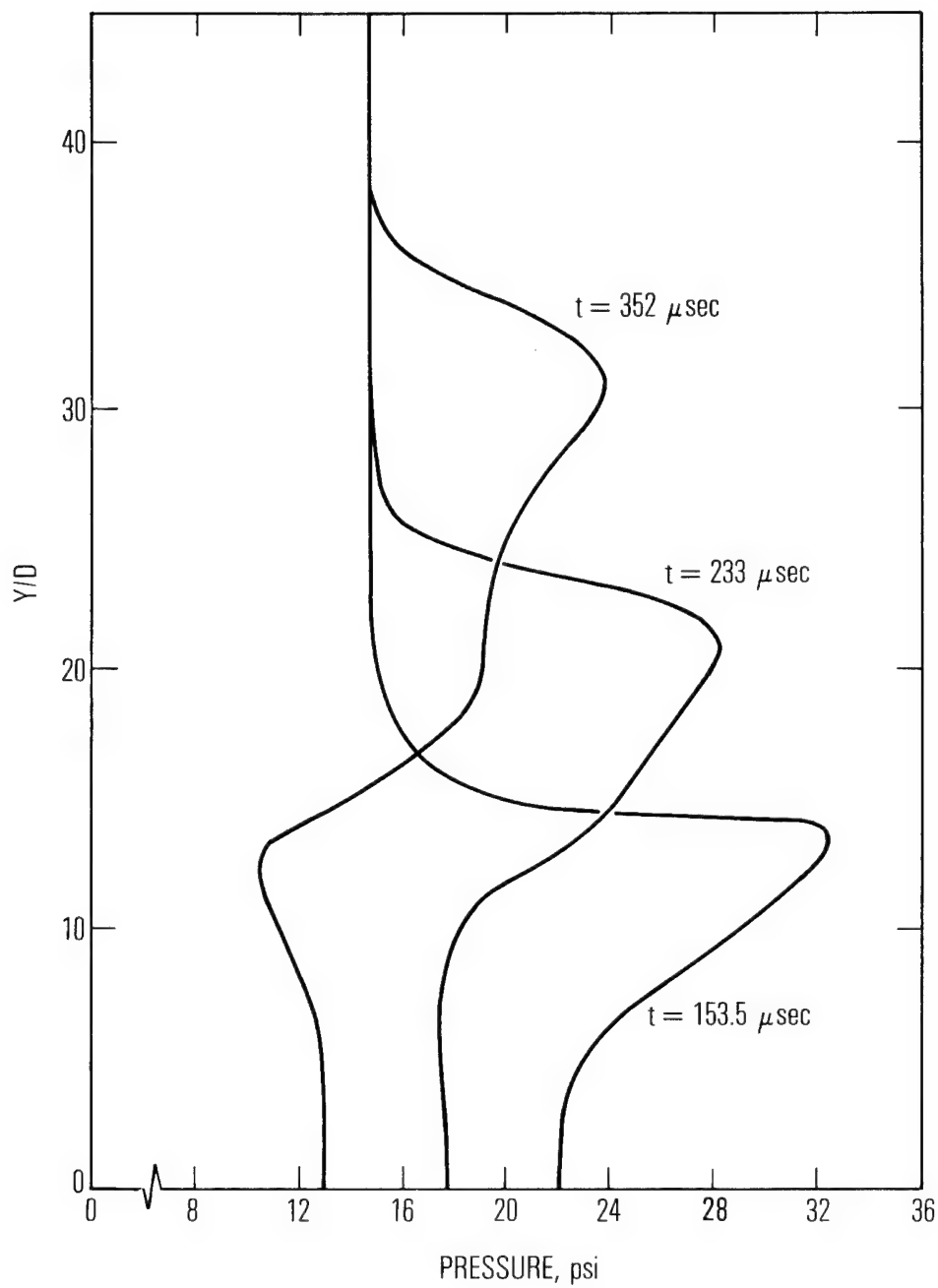


Fig. 8. Pressure Profile at $x/D = 5.2$

Figure 9 illustrates the velocity vector projections of the muzzle blast flow field at $t = 205 \mu\text{sec}$. The envelope of the outer blast can be located easily at $X/D \sim 31$ along the centerline. The Mach disc and the associated triple point position can be discerned as well [e.g., $(Y/D)_{\text{triple point}} \approx 11$].

The second computed results correspond to a 4.2-in. mortar. The initial conditions inside the barrel are $p = 1300 \text{ psi}$, $U = 900 \text{ ft/sec}$, and $T = 1700^\circ\text{K}$. The conditions outside the barrel are $p = 14.7 \text{ psi}$ and $u=v=0$. The projectile assumes a speed of 900 ft/sec . The calculations were performed with and without a projectile to determine the effect on the muzzle blast. The pressure and density contours for both cases are shown in Figs. 10 and 11. The results show that the existence of a projectile has a significant effect on the location of the blast along the centerline. However, its influence on the lateral development of the muzzle blast flow field is small. In Fig. 10, the approximate position of the projectile can be seen in the density contour.

It takes approximately 12 min on a CDC 7600 computer to integrate the governing equations to $t = 600 \mu\text{sec}$ with a 120×120 mesh system.

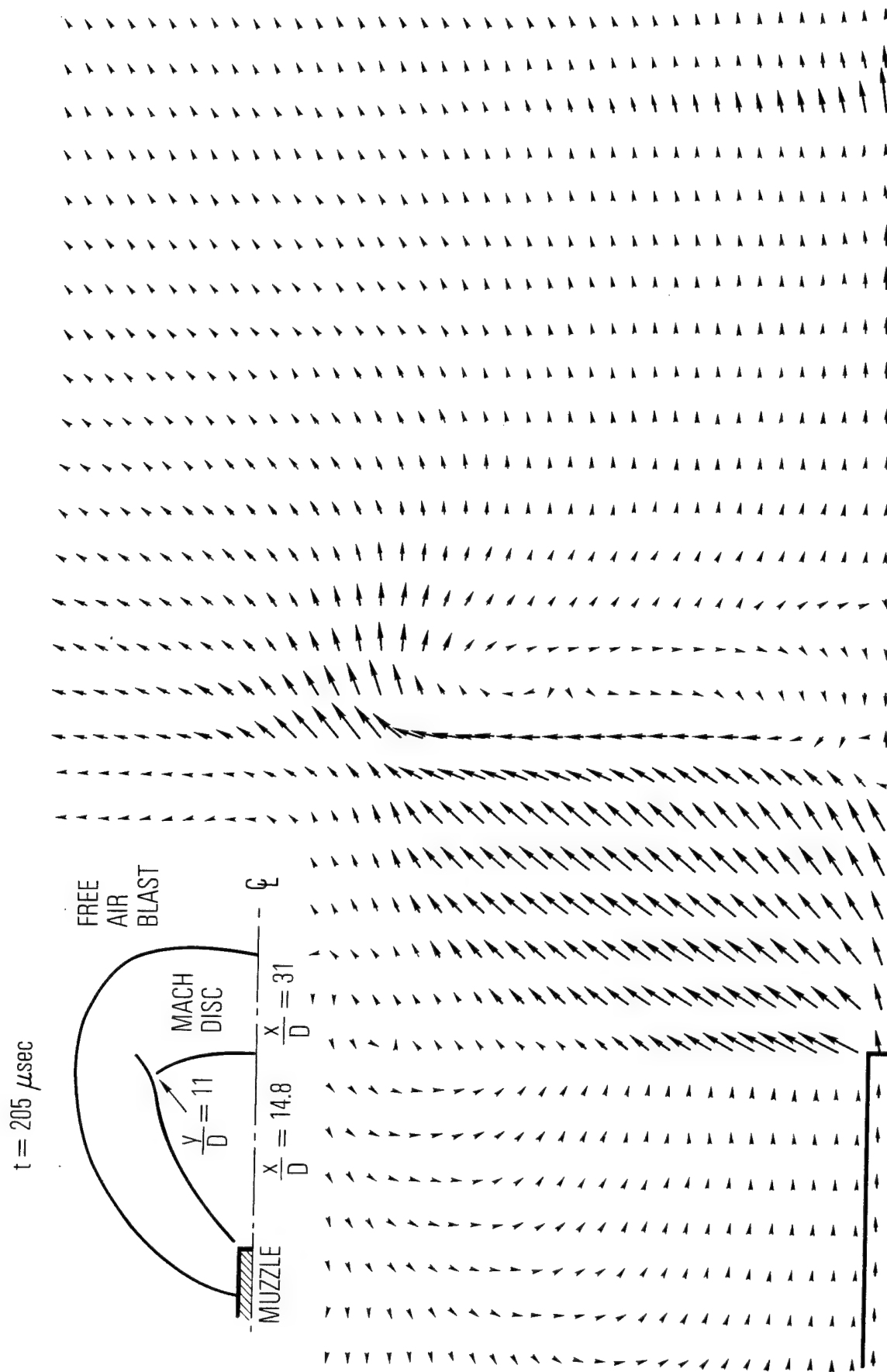


Fig. 9. Velocity Vector Projection

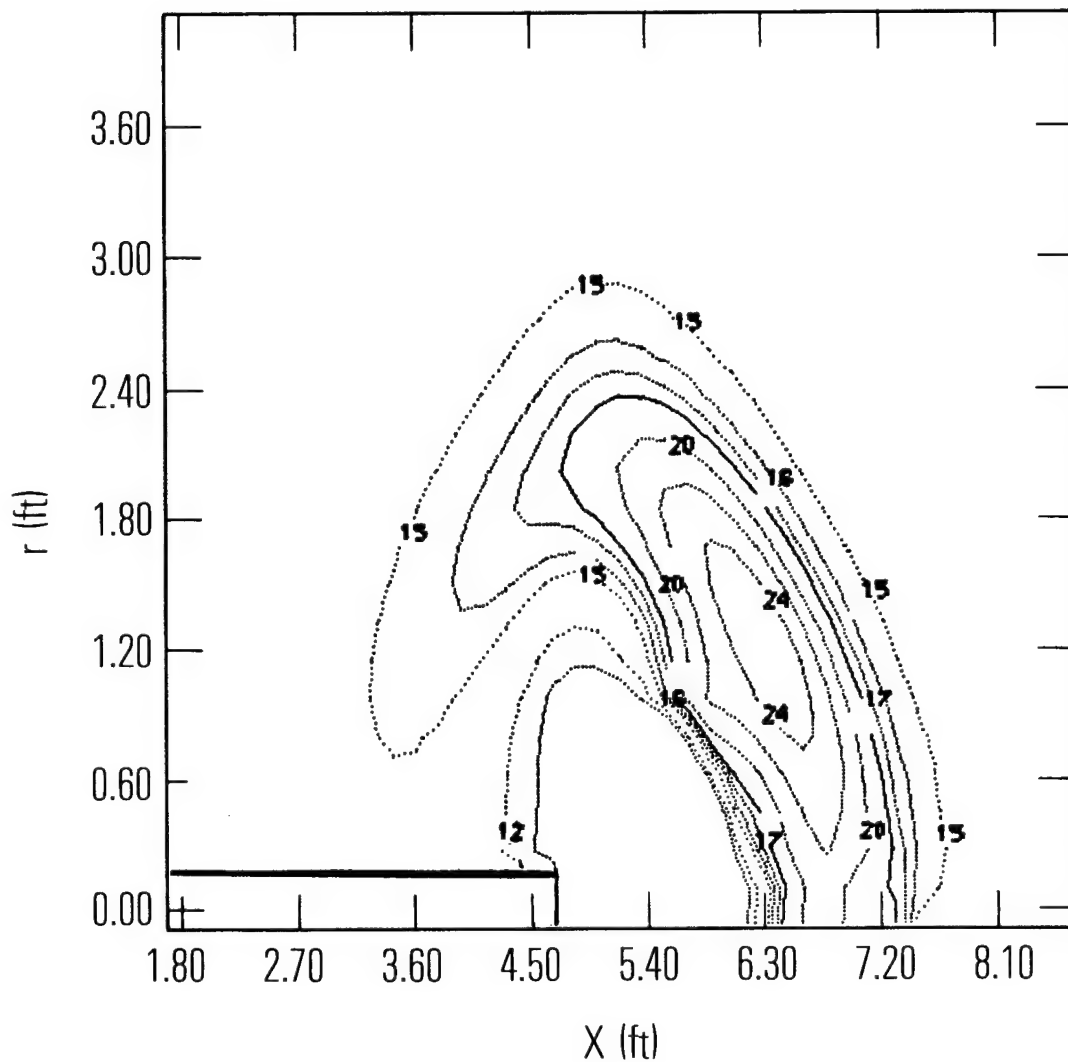


Fig. 10a. Constant Pressure and Density Profile for a 4.2-in.
Mortar with Shell [Pressure (Muzzle Blast)
 $T = 0.999E-03$]

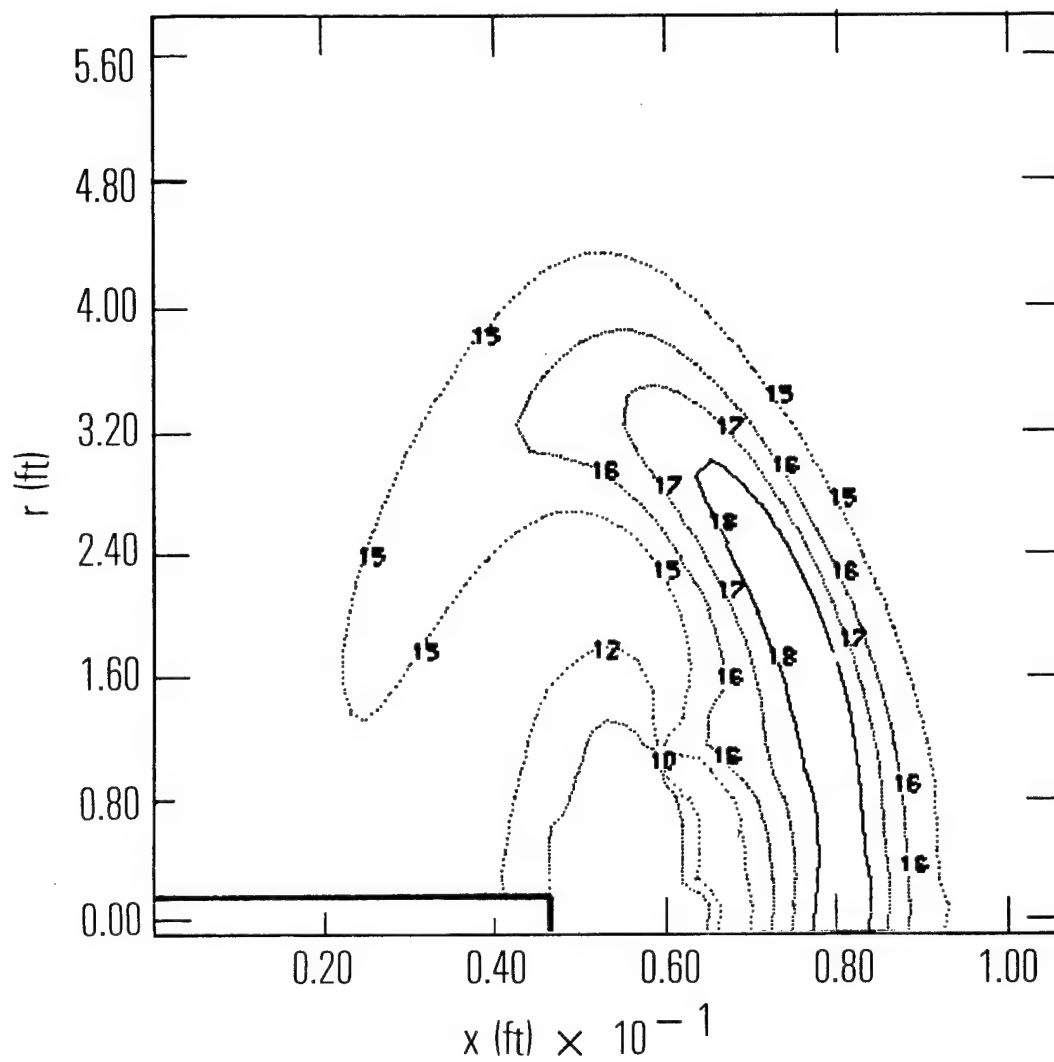


Fig. 10b. Constant Pressure and Density Profile for a 4.2-in.
Mortar with Shell [Pressure (Muzzle Blast)
 $T = 0.203E-02$]

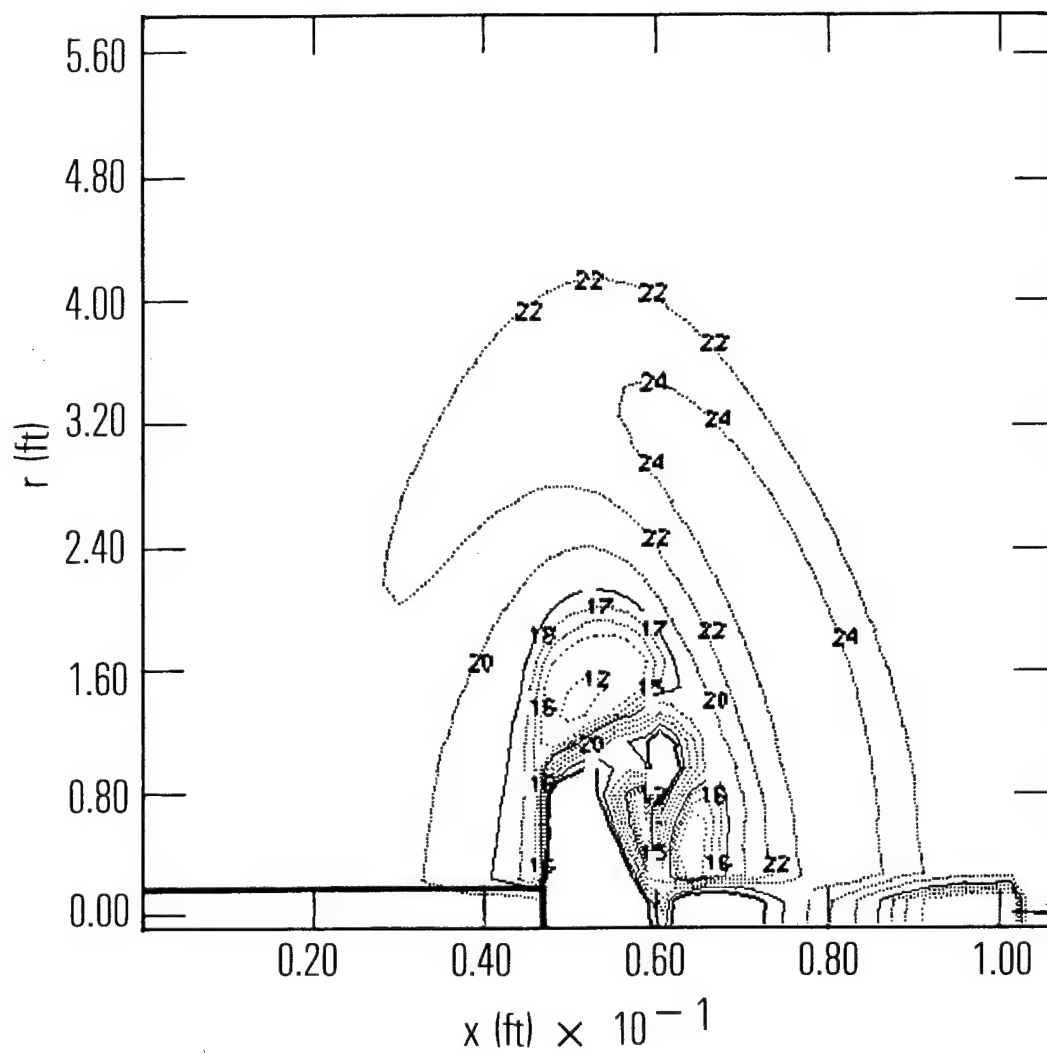


Fig. 10c. Constant Pressure and Density Profile for a 4.2-in. Mortar with Shell [$\rho \times 10^4$ (Muzzle Blast)
 $T = 0.203\text{E-}02$]

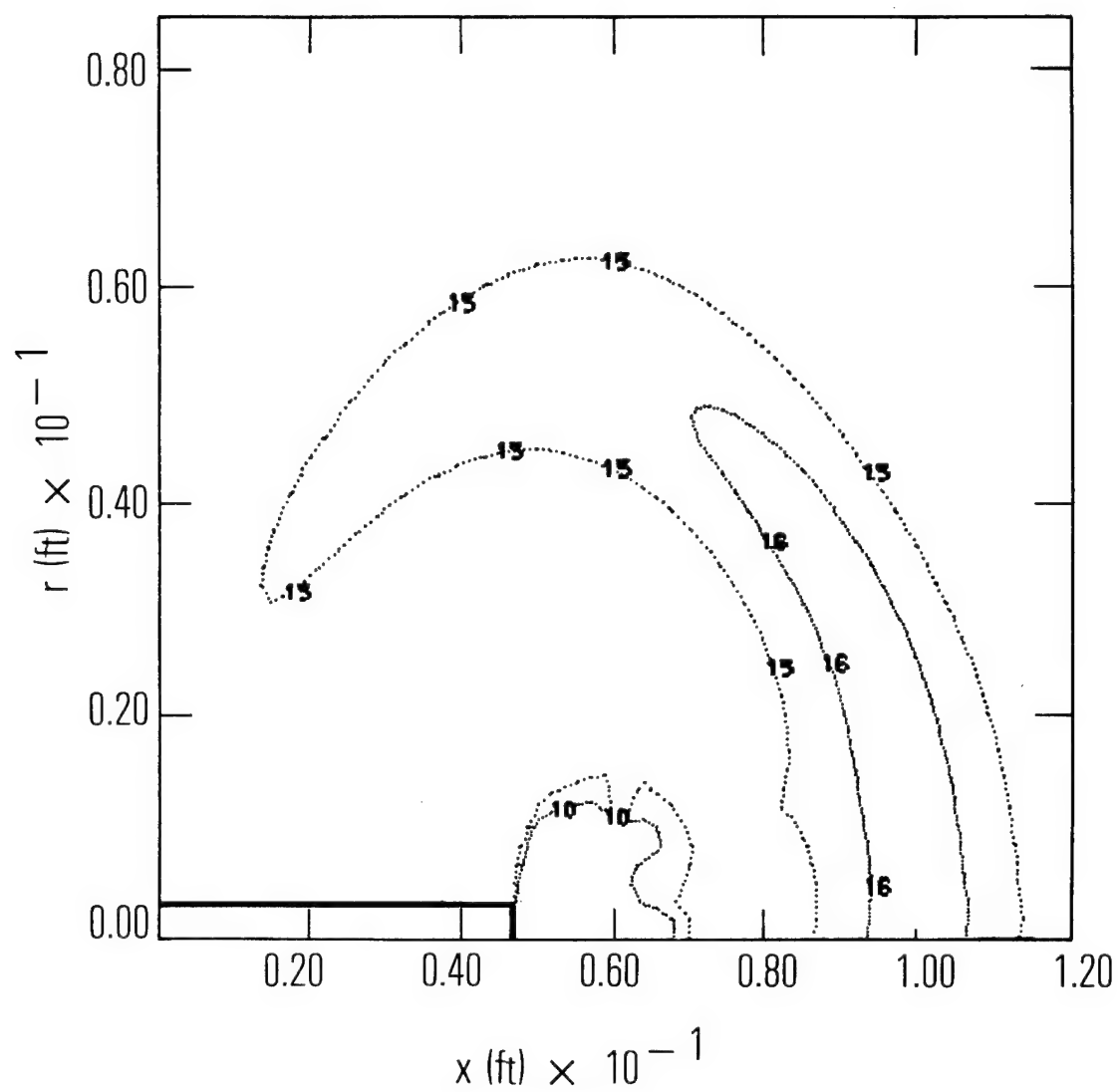


Fig. 10d. Constant Pressure and Density Profile for a 4.2-in.
Mortar with Shell [Pressure (Muzzle Blast)
 $T = 0.364E-02$]

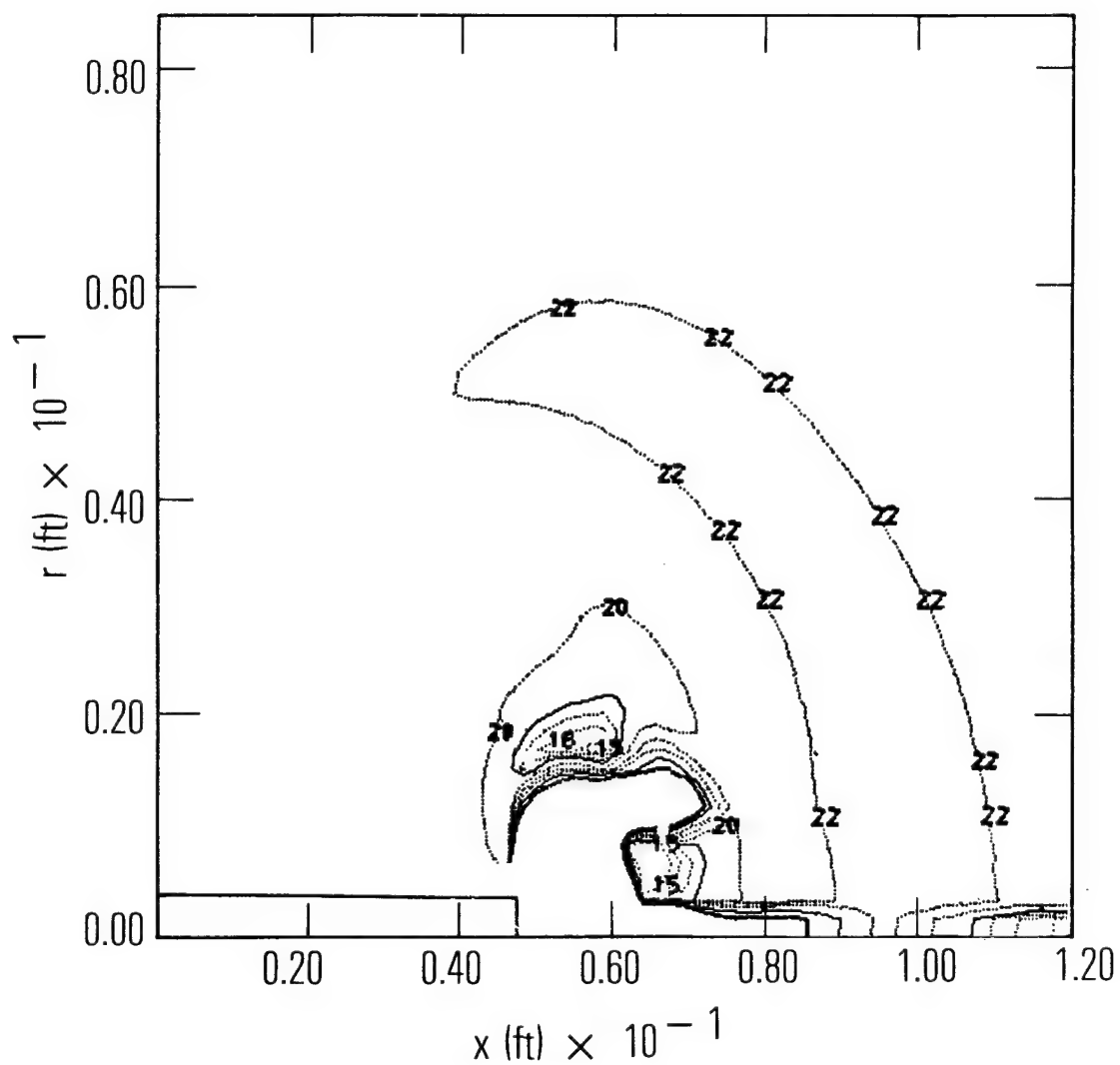


Fig. 10e. Constant Pressure and Density Profile for a 4.2-in. Mortar with Shell [$\rho \times 10^4$ (Muzzle Blast)
 $T = 0.364\text{E-}02$]

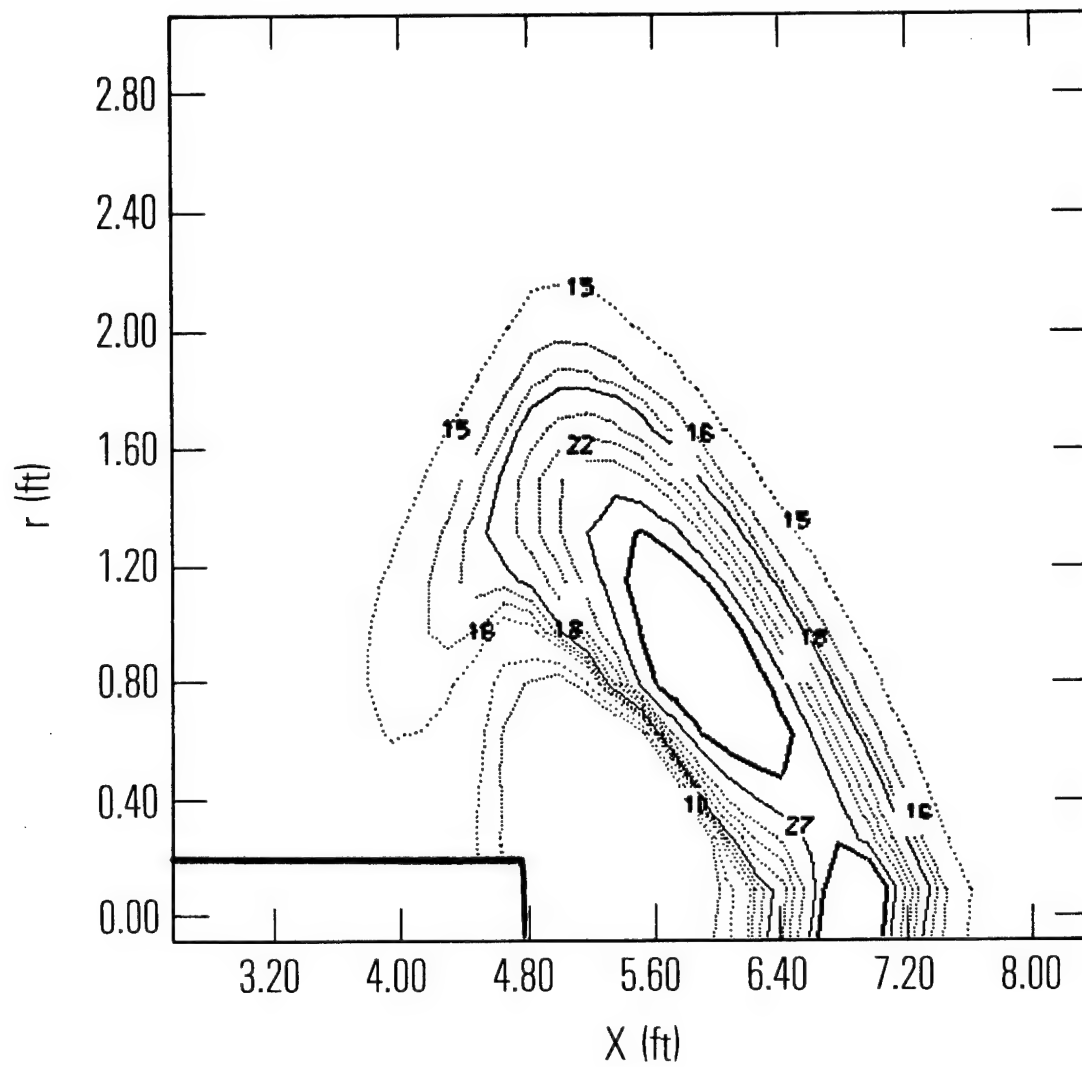


Fig. 11a. Constant Pressure and Density Profile for a 4.2-in.
Mortar with No Shell [Pressure (Muzzle Blast)
 $T = 0.552E-03$]

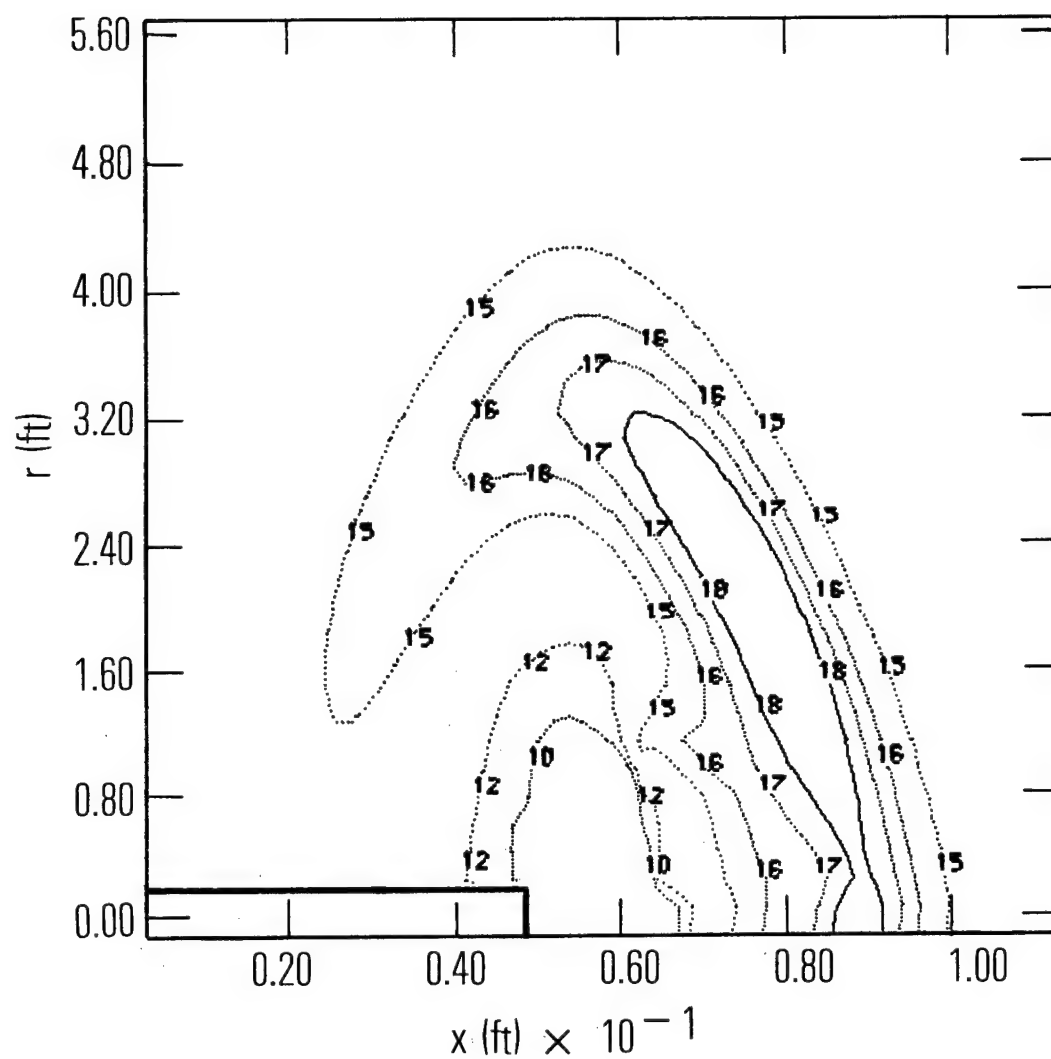


Fig. 11b. Constant Pressure and Density Profile for a 4.2-in. Mortar with No Shell [Pressure (Muzzle Blast)
 $T = 0.191E-02$]

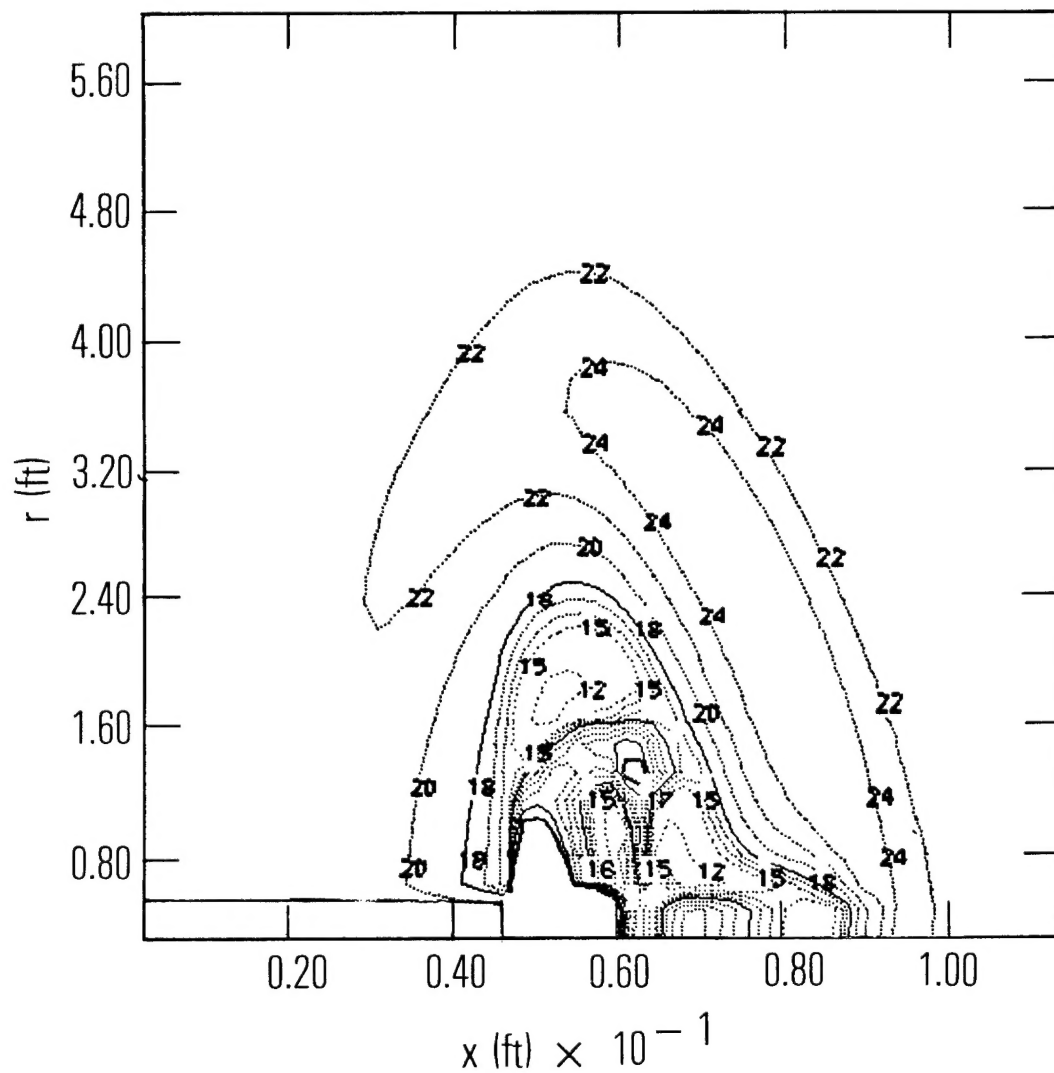


Fig. 11c. Constant Pressure and Density Profile for a 4.2-in. Mortar with No Shell [$\rho \times 10^4$ (Muzzle Blast)
 $T = 0.191E-02$]

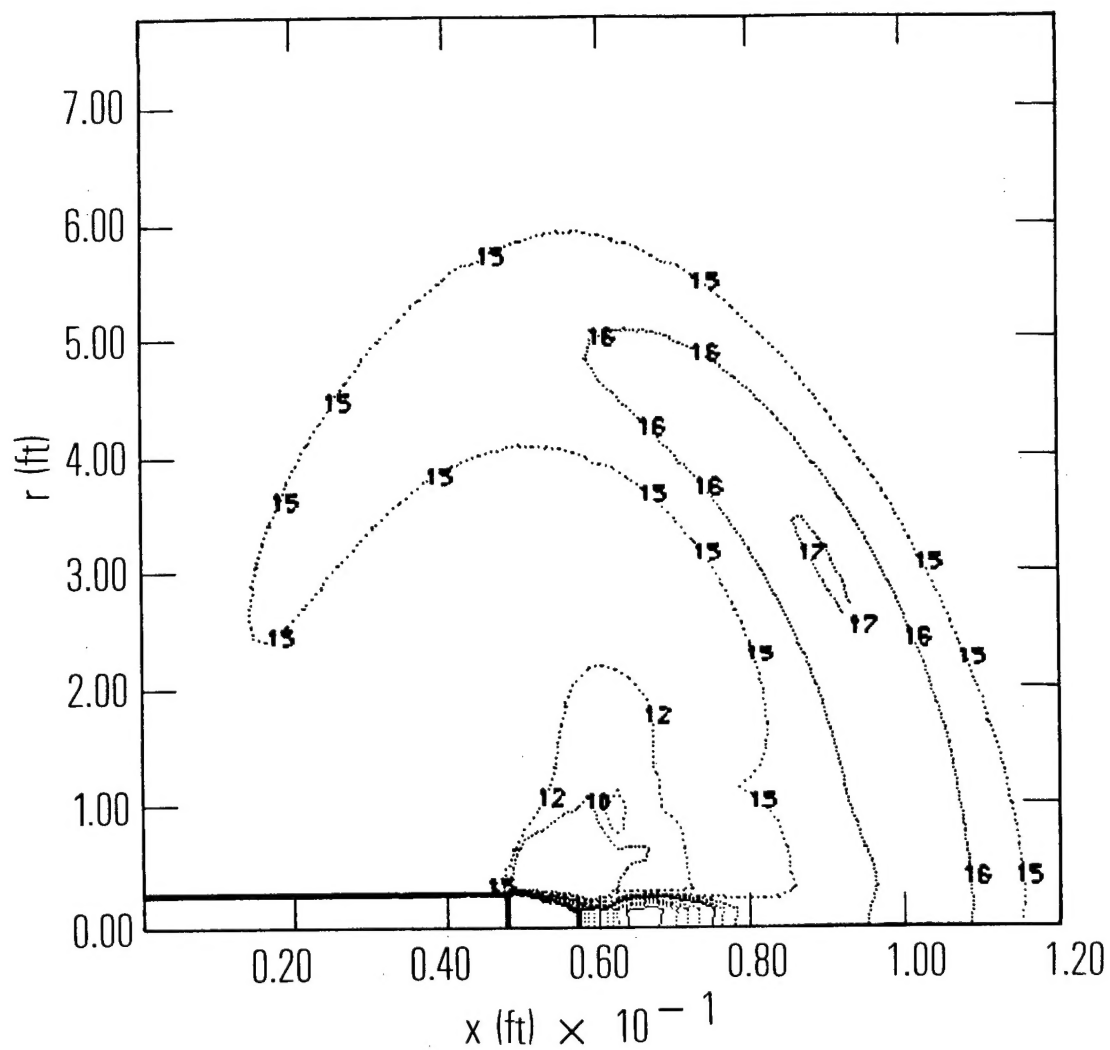


Fig. 11d. Constant Pressure and Density Profile for a 4.2-in. Mortar with No Shell [Pressure (Muzzle Blast)
 $T = 0.323E-02$]

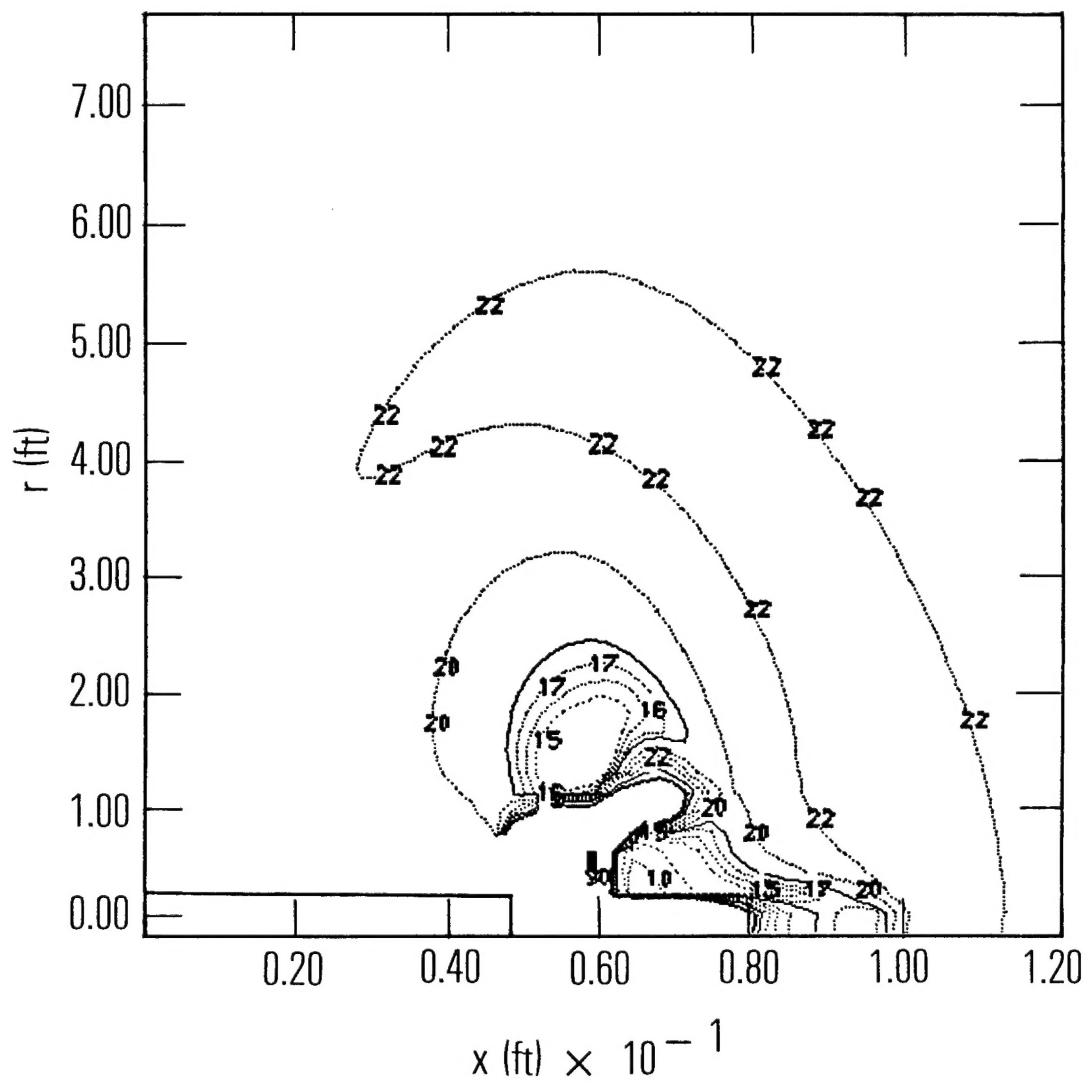


Fig. 11e. Constant Pressure and Density Profile for a 4.2-in. Mortar with No Shell [$\rho \times 10^4$ (Muzzle Blast)
 $T = 0.323\text{E-}02$]

4. SUMMARY

A numerical model, which uses Godunov's nonlinear scheme, is formulated to solve the time-dependent axisymmetric muzzle blast flow fields. Results are given for an M-16 rifle and a 4.2-in. mortar. The calculated results, including the effects of a shell, are compared with Schmidt's data, and the agreement is encouraging. Since the flow patterns are complex (consisting of outer blast wave, Mach disc, contact surface, jet shock, and large expansion fans), our numerical model with a simple shock smearing scheme works well. This good agreement is not considered to be fortuitous. We consider that it results from using Godunov's scheme which has properly taken into account the waves propagation and domain of dependence principle.